Strengthening protected areas for climate refugia on the Tibetan Plateau, China

Abstract

Protected areas (PAs) are at the forefront of efforts to conserve and restore biodiversity. However, there are risks that climate change can compromise the ecological benefits of PAs. Therefore, targeting conservation and adaptation efforts necessitate a well-understand of the relationship between PAs and climate refugia, defined as the regions that can buffer the impact of climate change. Recent attempts to identify climate refugia were primarily based on terrain-mediated features or climatic velocity, which ignore the ecosystem's internal processes. This work identified climate refugia on the Tibetan Plateau (TP), an amplifier of drastic global climate warming based on environmental diversity, phenology stability, and climatic velocity. It highlights the capacity to cope with extreme weather events, synchronization with plant growth cycles, and future climate adaptation, respectively. The results show that the distribution of climate refugia using different environmental diversity indicators (e.g., vegetation and topography) vary slightly but differs substantially from the priorities using phenology stability and climatic velocity. For instance, the high distribution probability of climate refugia derived from environmental diversity and climatic velocity is mainly concentrated at low (< 3000 m) or high elevations (> 6000 m), while the one using phenology stability is mainly observed at 3000m – 3800m. The inconsistent distribution of different types of climate refugia weakens the potential of functional complementarity. The existing nature reserves, the primary type of PAs in China, have critical conservation gaps in different types of climate refugia, indicating the urgency of incorporating climate refugia into PAs conservation planning on TP. Our work could help inform local conservation policies and improve the effectiveness of PAs.

Keywords Protected areas; Climate refugia; Nature reserves; Tibetan Plateau; Biodiversity; Conservation planning

1 Introduction

Protected areas (PAs) are the mainstream and extensive solution for conserving and restoring biodiversity by limiting human impacts (Gonçalves-Souza et al., 2021). However, many PAs are experiencing rapid climate change (Hoffmann et al., 2019; Asamoah et al., 2021; Dobrowski et al., 2021), which is a major threat to biodiversity and hampers PA's core objective (Garcia et al., 2014; Pecl et al., 2017; Hoffmann et al., 2019). Climate refugia, defined as buffer regions for species against exposure to changes in climatic conditions, are expected to mitigate the climate change impact on biodiversity and reinforce the PAs' effectiveness (Ashcroft, 2010; Keppel et al., 2012; Meddens et al., 2018). Consequently, identifying and safeguarding such climate refugia is increasingly acknowledged as a critical component of biodiversity conservation (Groves et al., 2012;

Carrol et al., 2017).

The importance of climate refugia has been widely demonstrated, although the approach by which they are identified is diverse (Ashcroft et al., 2012). In general, environmental diversity and climatic velocity are the two main criteria. For instance, areas of high environmental diversity (i.e., high spatial variability of some environmental variables, such as topography, and vegetation) can be delineated as potential refugia because they provide various resources, habitats, and microclimatic conditions (Oliver et al., 2010; Carrol et al., 2017), enhancing the resilience to external disturbance (Malika et al., 2009). Climatic velocity assesses the proximity and accessibility of future suitable climate conditions for species (Loaries, 2009). Areas with reduced climatic velocity can serve as refugia because species can track the changes in climate by moving short distances (Carrol et al., 2017). Many cases have used these criteria for climate refugia identification, particularly in North America (e.g., Carroll et al., 2017; Michalak et al., 2018; Stralberg et al., 2020).

Internal ecosystem processes have received scant consideration in identifying climate refugia despite their potential significance (Stralberg et al., 2020). For instance, vegetation phonology stability can reflect the synchronism between the plant growth cycle and animal behaviour, such as foraging, hibernation, and reproduction (Menzel et al., 2006; Reed et al., 2013). Climate refugia identified using various approaches may form useful complementarities regarding climate adaptation capacity and scale-dependent (Carrol et al., 2017). Furthermore, recent works suggested that planners should consider a variety of alternative metrics to overcome the shortcomings of individual approaches (Gillson et al., 2013; Garcia et al., 2014). Therefore, to promote biologically meaningful climate adaptation solutions, efforts need to be made to incorporate internal and external ecological processes to improve climate refugia identification (Brito-Morales et al., 2018) and understand the refugia distribution identified by multiple approaches (Michalak et al., 2020).

Incorporating climate refugia into PAs conservation planning can potentially increase PAs conservation effectiveness (Michalak et al., 2020). Furthermore, protecting climate refugia sites will help managers gain time to develop long-term adaptation strategies (Morelli et al., 2016). However, comprehensive and comparative studies on PAs' coverage and evolution of climate refugia using different approaches are still lacking.

An ideal area to explore these aspects is the Tibetan Plateau (TP) in China, which is located in two crucial global biodiversity hotspots (the Mountains of Southwest China and the Himalayas) (Myers et al., 2000). The region is highly sensitive to climate disturbance, and accelerated climate change risks jeopardize biological conservation efforts (Kuang & Jiao, 2016). Over the past decades, the Chinese government has gradually established several nature reserves (NRs, the primary type of PAs), forming a dense PAs network to protect these sensitive ecosystems. However, there is a growing concern about these PAs' conservation status and effectiveness (Li et al., 2020; Hua et al.,

2022). As climate refugia on the TP are still poorly understood, their identification and distribution within PAs can favour more effective conservation policies.

The aim of this study is multifold: (1) to map the climate refugia based on different approaches; (2) to discuss the inconsistencies among various types of climate refugia; (3) to investigate the elevation gradient characteristics of climate refugia distribution; and (4) to identify the relationship between NRs and climate refugia.

2 Materials and Method

2.1 Study area

The TP includes Qinghai Province, Tibet Autonomous Region, and parts of four other provinces of Gansu, Xinjiang, Yunnan, and Sichuan. It is also known as "The Roof of the World". TP has an average elevation of over 4000 m above sea level. The annual precipitation spans from 1000 mm to 100 mm in the southeast, with annual temperatures ranging between 20 °C to − 5 °C (Sun et al., 2020). A warming trend, faster than the global average, was observed in TP in the previous decades (Kuang & Jiao, 2016). This can have negative impacts on habitats and valuable species.

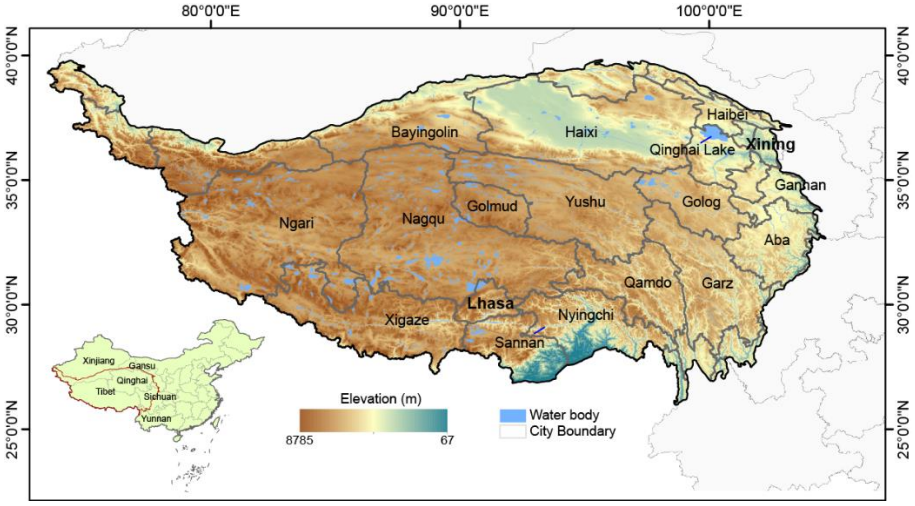

Figure 1. Study area location.

2.2 Data

To identify the climate refugia, we used enhanced vegetation index (EVI) derived from MOD13Q1 (250 m-resolution and 16 day-frequency) and land surface temperature (LST) from MOD11A2 (1 km-resolution and 8 day-frequency) from 2001 to 2020 (Tab. 1). We collected these datasets from Google Earth Engine (Gorelick et al., 2017) and selected only high-quality images according to the MODIS Quality Assurance flags. Also, we used a land cover dataset from MCD12Q1 with 500 m resolution and a digital elevation model (DEM) from Shuttle Radar Topography Mission with 90m resolution. We collected future climate data (annual mean temperature and annual precipitation) from WorldClim database generated from 8 CMIP6 global

climate models (BCC-CSM2-MR, CNRM-CM6-1, CNRM-ESM2-1, CanESM5, IPSL-CM6A-LR, MIROC-ES2L, MIROC6, and MRI-ESM2-0). Our dataset consisted of 53 NRs, representing approximately 40% of the total area currently covered by terrestrial NRs in China (Fig. S1).

Table 1. Data types and sources

Variables	Sources	Units	Period	Resolution	Website
TP boundary	Global Change Research Data Publishing and Repository	-	-	-	http://www.geodoi.ac.cn
China's prefecture administrative boundary		-	-	-	
NRs boundary	Resource and Environment Science and Data Center, Chinese Academy of Sciences	-	-	-	http://www.resdc.cn
DEM	SRTMDEM from Geospatial Data Cloud	m	-	90 m	http://www.gscloud.cn/
EVI	MOD13Q1	-	2001-2020	250 m	https://lpdaac.usgs.gov/products/mod13q1v006
LST	MOD11A2	K	2001-2020	1000 m	https://lpdaac.usgs.gov/products/mod11a2v006
Land cover	MCD12Q1	-	2010	500 m	https://lpdaac.usgs.gov/products/mcd12q1v006
Future climate	WorldClim database	°C/mm	2040-2060	2.5 minutes	https://worldclim.org/data/cmip6/cmip6climate.html

2.3 Assumptions of climate refugia

We assumed that regions with high environmental diversity, stable vegetation phenology, and reduced climatic velocity are suitable climate refugia for biodiversity. The reasons are the following. Environmental diversity metrics are a generalizable approach to identifying climate refugia. A heterogeneous environment (e.g., vegetation, topography, land cover) increases the resistance to climate change (Malika et al., 2009). Diverse ecosystems indicated the availability of a range of resources, as well as the existence of varied microclimatic conditions (Oliver et al., 2010). This is key to biodiversity and ecosystem stability through a variety of plant diversity and structure (Levin et al., 2007). Furthermore, high spatial variability of microclimates is key to the thermal shelter for different species within a small area (Keppel et al., 2012; Elsen et al., 2020, 2021). A global meta-analysis by Stein et al. (2014) found that species richness is associated closely with abiotic drivers such as topography, vegetation, land cover, and climate.

Many animals have periodic life behaviours that correspond with vegetation phenology. The high interannual vegetation phenology variability may negatively impact the availability of resources, with implications to animal survival needs (e.g., reproduction) (Menzel et al., 2006; Thackeray et al., 2010; Reed et al., 2013). Observational and experimental evidence showed that

phenological shifts reduce biodiversity and change regional species density (Plard et al., 2014; Wolf et al., 2017), pointing to the importance of stable vegetation phenology for biological conservation.

Climatic velocity is a function considering both the spatial and temporal gradient in climate variables in a particular location. It can be regarded as an initial rate at which species migrate to preserve stable climate conditions (Loarie et al., 2009; Hamann et al., 2015). Since the climate is a primary constraint to species distribution, they may be at risk of extinction when climate conditions to which they are adapted change quickly or disappear (Williams et al., 2007; Loarie et al., 2009). Therefore, it is possible to identify the potential exposure to climate shifts, which is key to measuring the exposure of organisms to climate change (IPCC, 2014) or identifying climate refugia (Carrol et al., 2017; Brito-Morales et al., 2018; Michalak et al., 2020).

2.4 Calculation of climate refugia indicators

2.4.1 Environmental diversity

We developed and compared five metrics of environmental diversity (elevation, landcover, EVI, summer LST, and winter LST) following Carroll et al. (2017) and Silveira et al. (2021). For EVI diversity, we constructed a composite image by generating the 90th percentiles of EVI from 2001 to 2020 with the selection of high-quality pixels using the Quality Assurance flags and vegetation layers of MCD12Q1. Using this approach, we reduced high EVI values' disturbance and obtained the EVI peak values (Farwell et al., 2020). The standard deviation (STD) of EVI composite images was then calculated using a moving window with a size of 5×5 pixels. The size of moving windows (5 pixels) is a compromise between animals' mobility in a short time and the data input amount for STD calculations. The STD value was allotted to the moving windows' center pixel. With this, we delineated the spatial diversity of EVI.

LST images were composited in summer and winter by using the median of all high-quality images available in summer and winter from 2001 to 2020, derived from MOD11A2. Using median rather than mean can minimize the effects of extreme high/low values and reduce cloud cover impacts (Elesen et al., 2020). Overall, two LST composited images for summer and winter were produced. Similarly, we calculated the STD within a moving window with a size of 5 pixels to represent the LST spatial diversity.

Similarly, we used the STD within a moving window with a size of 5 pixels to assess the elevation spatial diversity pattern. Land cover diversity was represented by Shannon's diversity index assessed with FRAGSTATS v4.2. We also used the moving window with a size of 5 pixels to match other calculations. The environmental diversity calculation just considered grasslands, cropland, and forests, since other land cover types do not provide the necessary food resource or have poor accessibility.

2.4.2 Phenology stability

We extracted the STD from 20 years (2001-2020) of vegetation phenology to describe the phenology stability. The extraction of vegetation phenology was based on EVI images from MOD13A1. First, we replaced the median of the uncontaminated EVI between November and March of the next year for the snow-contaminated EVI values during the non-growing season. This process was required to eliminate this snow-related influence during the non-growing season, in line with previous works (Ganguly et al., 2010; Zhang et al., 2006). We used the Savitzky-Golay filter to reconstruct the EVI series following Chen et al. (2004), and the grassland class of MCD12Q1 was used to determine the phenological calculation areas.

After data preprocessing, we used three widely accepted methods (Derivative method, Threshold method, RC_{max} method) to calculate two-phenology metrics for each year, namely the start date of the growing season (SOS) and the end date of the growing season (EOS) following Cong et al. (2012), Shen et al. (2014) and Zhang et al. (2018). The average of these phenology metrics was finally calculated as vegetation phenology. The average ensemble method can reduce the error of using a single method (Cong et al., 2017), and is also widely applied in the current phenological calculations, such as Shen et al. (2014), Cong et al. (2017), and Shen et al. (2022).

In the Derivative method (Fig. S2a), a rapid increase in EVI indicated active growth of vegetation. Therefore, the SOS/EOS is characterized as the day on which NDVI increases/decreases at the fastest rate in a year when the derivative of the EVI series [f'(t)] was the maximum/minimum (Studer et al., 2007). In the Threshold method (Fig. S2b), we firstly used the formula (1) to covert EVI series from each pixel to calculate EVI_{ratio}, and 50% was used as the threshold to determine the SOS and EOS according to local observations (White et al., 1997; Yu et al., 2010).

$$EVI_{ratio} = \frac{EVI_t - EVI_{min}}{EVI_{max} - EVI_{min}} \quad (1)$$

Where EVI_t is the EVI value at a given time *t*, and EVI_{min}, EVI_{max} is the annual maximum and minimum EVI values at this pixel, respectively.

In the RC_{max} method (Fig. S2c), we firstly used the formula (2) to obtain the rate of change (RC) of EVI. And the SOS/EOS was determined as the time when $EVI_{rc}(t)$ reached its maximum, following Piao et al. (2006) and Cong et al., (2012).

$$EVI_{rc}(t) = \frac{EVI_{t+1} - EVI_t}{EVI_t} \quad (2)$$

Where $EVI_{rc}(t)$ is the RC of EVI value at a given time *t* and EVI_t is the EVI value at a given time *t*.

Finally, the average of SOS generated by three methods was determined as the ultimate SOS (Fig. S2d). We chose SOS instead of EOS to calculate phenology stability, considering the reproductive needs of animals highlighted in Silveira et al. (2021). We computed the STD of SOS

among 20 years (2001-2020) for each pixel to quantify phenology stability.

2.4.3 Climatic velocity

The calculation of future climatic velocity was derived from dividing the temporal gradient of climate change (units: °C yr^{-1} for temperature and mm yr^{-1} for precipitation) by the spatial gradient of climate variability (units: °C km^{-1} or mm km^{-1}) and then obtaining the velocity variable (units: km yr^{-1}), as shown in formula (3).

$$V = \frac{Temporal\ gradient}{Spatial\ gradient} = \frac{°C \times year^{-1}}{°C \times km^{-1}}\ or\ \frac{mm \times year^{-1}}{mm \times km^{-1}} = \frac{km}{year} \quad (3)$$

Climate data from the WorldClim database for the current (1970-2000) and future (2041-2060) were used as input for calculation. Two extreme future climate scenarios: SSP1-2.6, SSP5-8.5 were considered. We used the average of the output from eight global climate models to describe the future climate condition since it can overcome a single model analysis's error. Additionally, we conducted a standard error estimate to map the uncertainty of future climate from 8 global climate models for each pixel (Fig. S3). The velocity calculation just considered grasslands, cropland, and forests, for other land cover types do not provide a necessary food resource or be poor accessibility. More detailed calculations about the climatic velocity can be consulted in Loarie et al. (2009).

2.5 Relationship among different climate refugia indicators

Spearman rank correlation was used to analyze the relationships among the different climate refugia indicators. We extracted the values of all refugia indicators based on about 5000 random points for analysis. We used the tool 'Create Random Points' of ArcGIS 10.5 to generate the random points, and the distance between random points is no less than 10 km. We hypothesized that regions with high environmental diversity, stable vegetation phenology, and slow climatic velocity could be climate refugia. Therefore, before the correlation analysis, the extracted values of phenology stability indicators (STD of SOS) and climatic velocity of precipitation/temperature were multiplied by -1 to guarantee a consistent interpretation of correlation coefficients. Statistical analysis was applied with Statistical Package for Social Science (SPSS) version 22.

2.6 Identification of priority climate refugia

The climate refugia priority areas were delimited by considering areas where each indicator is in the respective top 20%, referring to the determination of ecosystem services and biodiversity hotspots in the previous studies (Qiu et al., 2013; Xu et al., 2017; Li et al. 2020). This follows the assumption that regions with high environmental diversity, stable vegetation phenology, and reduced climatic velocity are suitable climate refugia. Therefore, 20% of the areas with the highest values were designated as priority areas for environmental diversity indicators, and 20% of regions with the lowest values were determined for phenology stability indicators and climatic velocity indicators. We also conducted a sensitivity analysis on other thresholds (15%, 25%, 30%) to identify

priority areas and explore the analysis's robustness.

To assess the climate refugia pattern along the elevation gradient, we calculated the distribution probability of climate refugia in each 100 m interval. This is expressed as the pixels' proportion identified as climate refugia within the elevation interval of 100 m. Locally weighted regression (LWR) was used to fit the distribution probability.

2.7 Analysis of coverage of NRs to climate refugia

NRs' boundary was introduced to identify the conservation gaps between the NRs and climate refugia identified by 8 indicators, using a spatial overlap analysis. If the climate refugia were identified within the NRs relative to its total area (i.e., coverage of NRs to climate refugia) being above the NRs proportion of the TP, the NRs had a good conservation status for climate refugia. Otherwise, the existing NRs in the TP had poor conservation. We also analyzed the proportion of climate refugia identified in NRs. NRs consist of three parts: 1) strictly-protected core zones, 2) buffer zones with limited scientific observation, 3) and experimental zones. The proportion of climate refugia in different components of the NRs was also analyzed.

3 Results

3.1 Inconsistency among the climate refugia indicators

High-value regions of different refugia indicators showed different patterns (Fig. S4). In general, high values of environmental diversity indicators were mainly distributed in the southeast of TP (Fig. S4a-e). The land cover diversity with high value was mostly concentrated in the southeastern areas with dense forests and shrubs (Fig. S4c). SOS's low-STD (i.e., stable phenology) region was scattered over the vegetative land (Fig. S4f). The regions with low precipitation velocity (Fig. S4g) were mainly distributed in the south of the TP, including Xigaze, Sannan, Nyingchi, and the low temperature-velocity regions (Fig. S4h) were concentrated in the south and southeast of the study area (e.g., Sannan, Nyingchi, Qamdo, Garz).

Spearman's rank correlation analysis shows that the climate refugia indicators have an inconsistent pattern, especially phenology stability (Fig. 2). For example, summer LST diversity showed a weak positive correlation with all other environmental diversity indicators and climatic velocity. All correlation coefficients were all lower than 0.16. According to significantly negative or low correlations, the differences between phenology stability (i.e., SOS) and diversity/climatic velocity indicators were greater than any contrast among the diversity/climatic velocity indicators. For example, there was a significant negative correlation between phenological stability indicator (i.e., SOS) and land cover diversity with a correlation coefficient of -0.32 ($p<0.05$), and a weak negative correlation with other environmental diversity/ climatic velocity indicators. Elevation diversity, winter LST diversity, and precipitation and temperature velocity formed a group of closely correlated metrics, with all the correlation coefficients being greater than 0.34 ($p<0.05$). Overall, an

inconsistency was observed among these climate refugia indicators, especially between the phenology stability indicator and the other two categories of indicators (i.e., environmental diversity and climatic velocity).

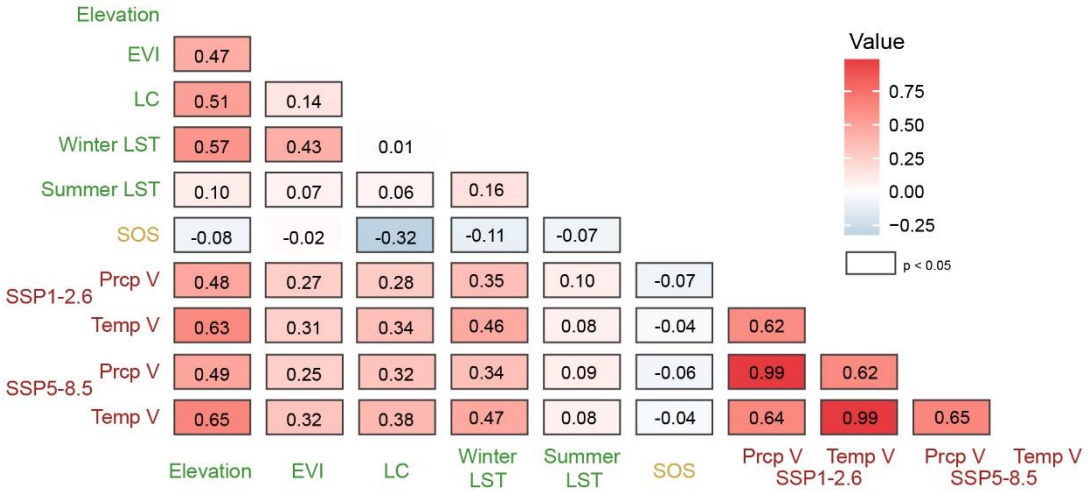

Figure 2. Spearman correlation coefficient among climate refugia indicators. The colour shade represents the correlation coefficient. The thick border of the box is used to indicate the significance ($p < 0.05$). Green labels are environmental diversity indicators, the orange label is phenology stability indicator, and red labels are climatic velocity indicators. Land cover (LC), land surface temperature (LST), climatic velocity (V), precipitation (Prcp), temperature ("Temp") and start of the growing season (SOS).

3.2 Distribution of priority climate refugia

The priority areas for climate refugia are mainly concentrated in the eastern and southern parts of the TP (Fig. 3). There is a clear distinction between the northwest and southeast areas. In terms of elevation diversity, priority areas were mainly distributed in the southeast of TP (Fig. 3a). This pattern is consistent with other priority regions based on EVI (Fig. 3b), winter LST (Fig. 3d), summer LST (Fig. 3e), and temperature velocity (Fig. 3h, j). Regarding landcover diversity, priority areas are concentrated in the southeast of the study area (e.g., Sannan, Nyingchi, Garz, and Aba) (Fig. 3c). The priority regions based on SOS stability are mostly distributed in the eastern TP, including the surrounding regions around Qinghai Lake (Fig. 3f). There is a small distribution in the middle of the study area (e.g., Nagqu, Golmud, and Yushu), however different from the previous. Besides, the priority regions based on precipitation velocity are mainly distributed in Xigaze and have finite distribution in several southeastern cities such as Nyingchi, Qamdo, and Garz (Fig. 3g, i).

The results indicate that the distribution of climate refugia identified using different environmental diversity indicators vary slightly from each other, particularly in landcover diversity

(Fig. 3c), but differed substantially from the priorities using phenology stability (Fig. 3f) and climatic velocity (Fig. 3g-j). This confirmed the observed in Fig. 3. According to the sensitivity test, the different thresholds to determine the priority climate refugia (15%, 25%, 30%) showed a relatively similar pattern (Fig. S5-S7).

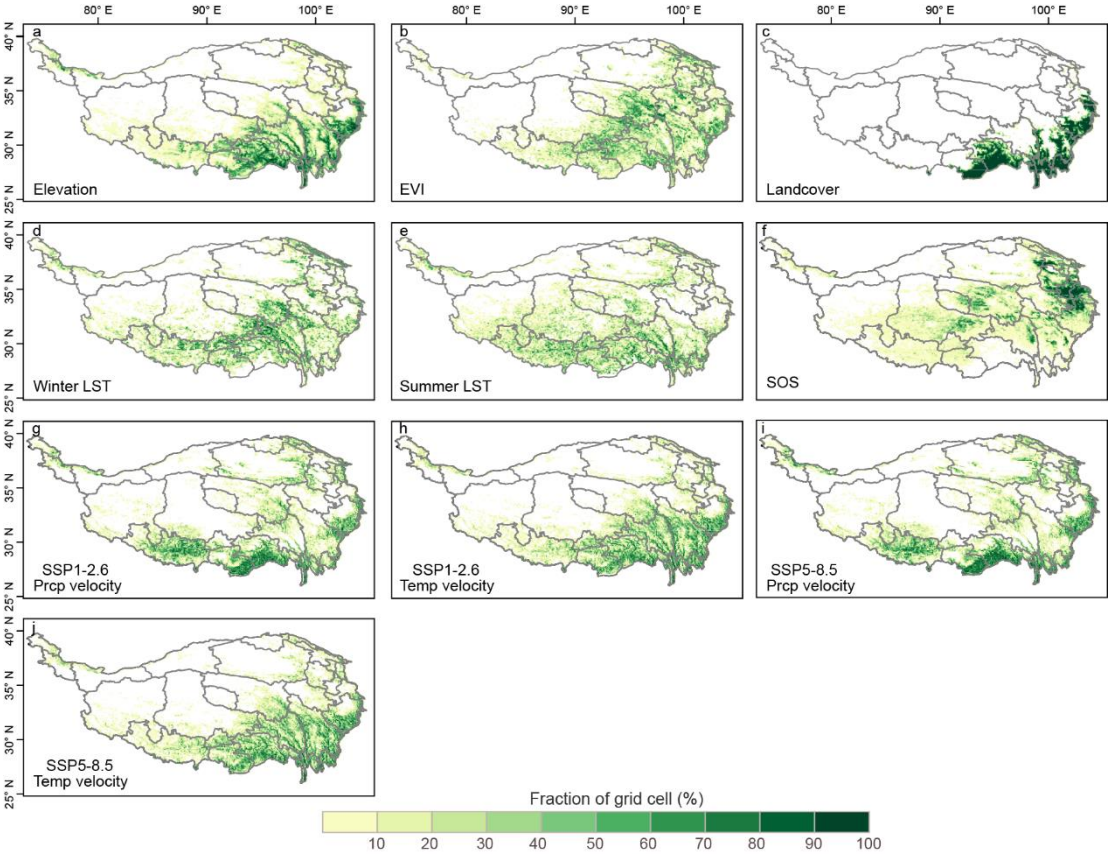

Figure 3. Distribution of priority climate refugia based on different indicators (%). The figures are aggregated to 0.1-degree resolution for improved visualization. The colour shade green represents the percentage of priority climate refugia. Grey lines represent the municipal administrative boundary. (a-e) showed the environmental diversity of elevation, EVI, landcover, winter LST and summer LST, (f) showed the phenology stability indicator, and (g-j) showed the future climate change velocity for precipitation and temperature for SSP1-2.6 and SSP5-8.5, respectively. Enhanced vegetation index (EVI), land surface temperature (LST), the start of the growing season (SOS), precipitation (Prcp), and temperature (Temp).

3.3 Contrasting relationship of priority climate refugia to elevation

Fig. 4 shows the distribution probability of different climate refugia indicators along the elevation gradient. Elevation diversity, two future climatic velocities (precipitation and temperature) indicators showed a similar trajectory, with a high probability at low elevation and high elevation, and low probability at medium elevation. The distribution probability increased gradually when the

elevation was above 4800 m, which matched the winter LST pattern. This suggested that, at least in the TP, the highest mountain area and low-elevation regions are most topographically diverse. The probability of SOS and EVI presented a symmetrical distribution along the axis of 3600 m. Land cover diversity has a very high probability of distribution below 2000 m but then decreases rapidly with the increasing elevation.

The high distribution probability of terrain-based/velocity-based indicators is concentrated in low (<3000 m) and high elevations (>6000 m). The probability derived from the phenology stability indicator (SOS) performed the best between 3000 m and 3800 m (Fig. 4). This inconsistency emphasized that different climate refugia indicators may differ in some elevation ranges (e.g., <2000 m and > 4800 m).

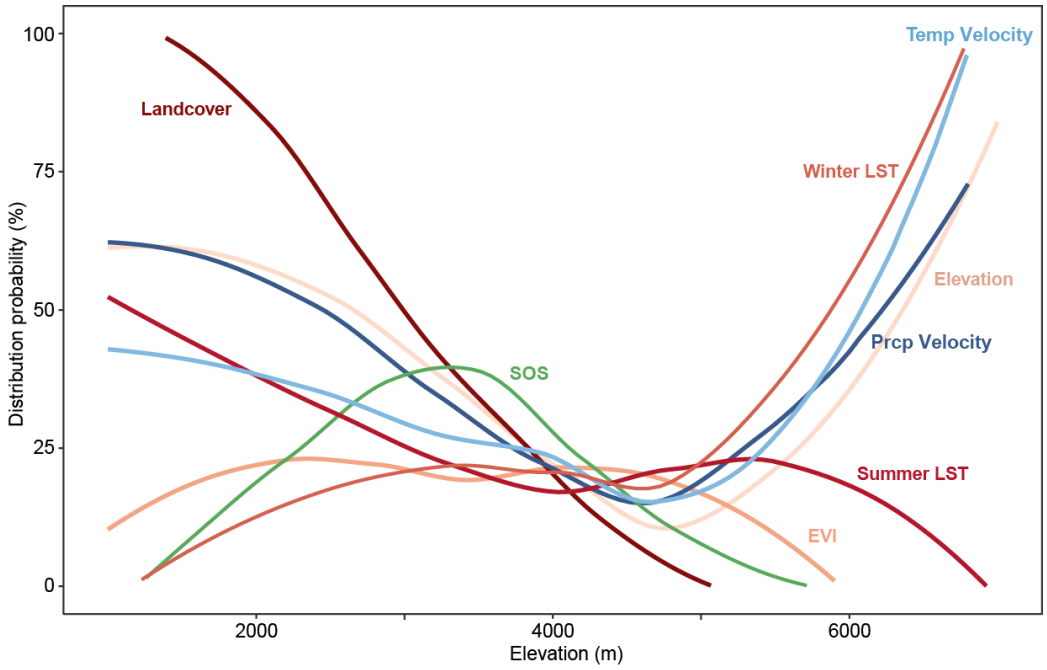

Figure 4. Climate refugia distribution probability in their relationship with elevation. Land surface temperature (LST), precipitation (Prcp), and temperature (Temp), start of the growing season (SOS), and enhanced vegetation index (EVI).

3.4 Relationship between NRs and priority climate refugia

TP's NR has a low coverage for the prior climate refugia based on different indicators (Fig. 5). Compared to NRs' 27.3%, TP total land surface contributions to climate refugia are, on average 15.3% for environmental diversity, 16.1% for climatic velocity, and 25.2% for phenology stability. Among different environmental diversity indicators, the maximum coverage percentage was observed in EVI diversity (19.4%), and the minimum is 9.9% for landcover diversity. Regarding climatic velocity, current NRs covered 15.4% (15.5%) of priority regions with precipitation velocity and 11.6% (11.8%) for temperature velocity under SSP5-8.5 (SSP1-2.6). Phenology stability showed a higher coverage (25.2%) than the previous.

The above patterns still hold if considering the proportion of climate refugia in NRs. On average, 13.0% of the NRs can be considered climate refugia based on different indicators. The maximum proportion was observed in SOS stability (17.8%), and the minimum (7.3%) for landcover diversity. Even the core zones of NRs have a relatively low proportion of climate refugia (Fig. S8). These results highlighted that climate refugia within the NRs are also limited.

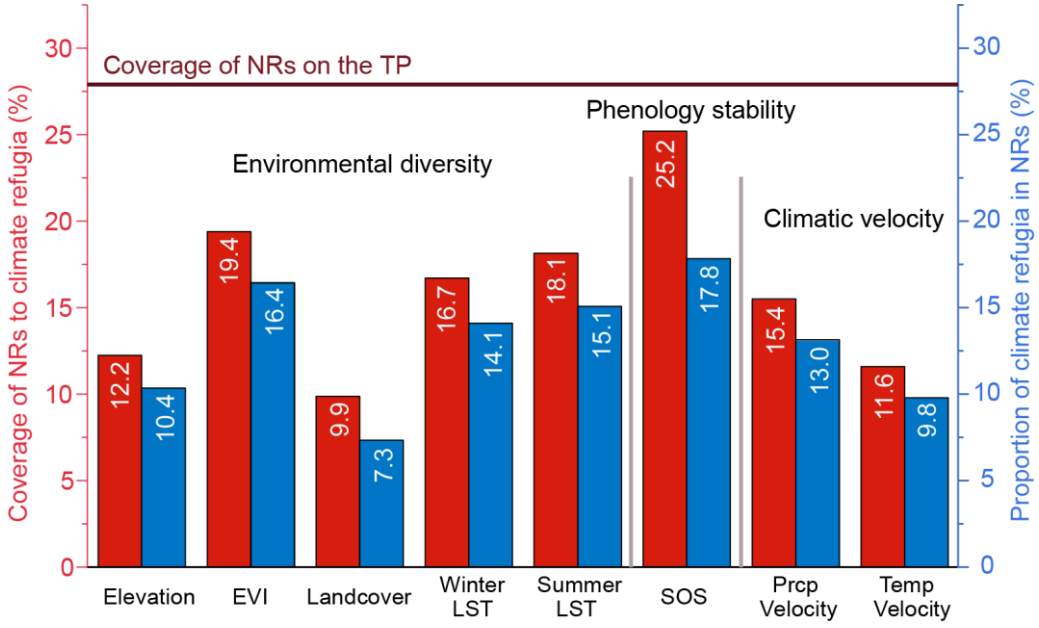

Figure 5. Coverage of NRs for climate refugia and proportion of climate refugia in NRs. The red bar means the coverage of NRs to climate refugia (%) and the blue bar means the proportion of climate refugia in NRs (%). The dark red line is the coverage rate of NRs on the TP, which is 27.3%. Only climatic velocity under SSP5-8.5 was showed because the situation in SSP1-2.6 is very similar to that in SSP5-8.5. Land surface temperature (LST), precipitation (Prcp), temperature (Temp), start of the growing season (SOS), and enhanced vegetation index (EVI).

The coverage of NRs on the TP experienced an increase of 15.2 percentage points between 1990 and 1995. However, the coverage of NRs for climate refugia was not substantially increased correspondingly in all eight refugia indicators during this period (Fig. 6a-c). After 1995, the unbalanced growth between NRs and climate refugia improved. For instance, compared with the 6.5 percentage point increase in the Rs coverage on the TP between 1995 and 2000, SOS coverage and EVI increased by 14.9, and 11.1 percentage points, respectively. This showed that with the expansion of NRs, the coverage of NRs to climate refugia also increased.

Although national-level NRs expanded rapidly from 2000 to 2005, the coverage for climate refugia did not attain the expansion rate of national-level NRs, except for SOS (Fig. 6d-f).

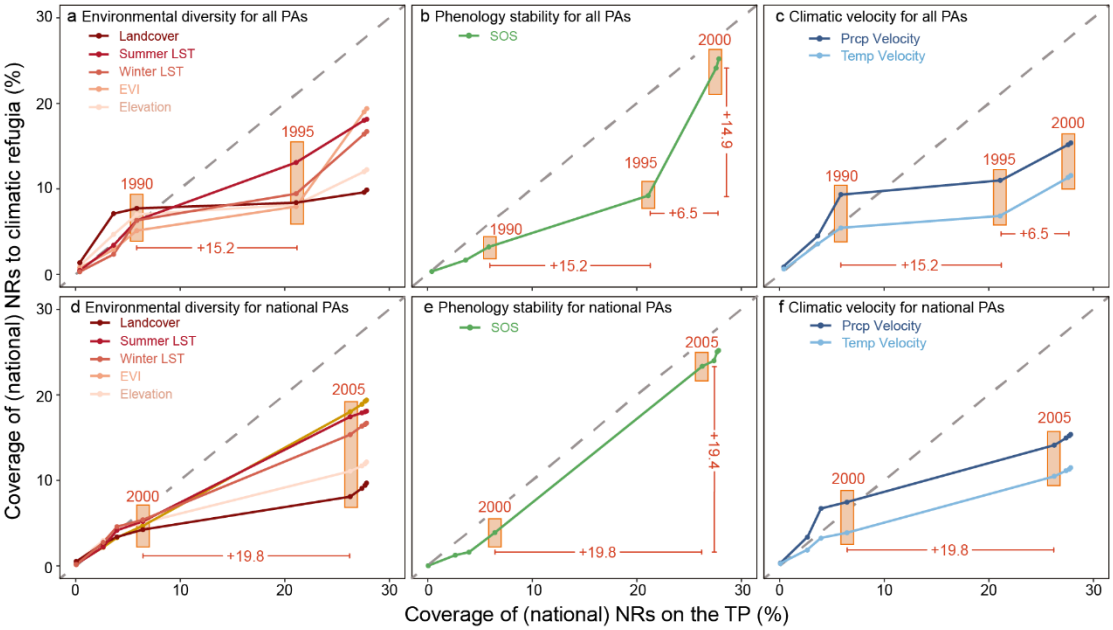

Figure 6. The evolution process of NRs and their coverage for climate refugia. Two types of NRs were considered: (a-c) for all NRs and (d-e) for national NRs. The grey dotted line is the 1:1 line. The orange rectangle was used to label key time nodes, and the red font was used to label the growth rate of coverage (units: percentage points). Only climatic velocity under SSP5-8.5 was showed because the situation in SSP1-2.6 is very similar to that in SSP5-8.5. Land surface temperature (LST), precipitation (Prcp), and temperature (Temp), start of the growing season (SOS), and enhanced vegetation index (EVI).

4 Discussion

4.1 Inconsistent distribution limits functional complementarity of various climate refugia

The adaptation capacity of climate refugia, mapped by different indicators, is different (Fig. 7). For instance, climate refugia derived from environmental diversity are aimed at tackling extreme weather events (Keppel et al., 2012; Elsen et al., 2020, 2021; Silveira et al., 2021). Their distribution largely depends on the neighbourhood's topographic characteristics. Those derived from climatic velocity emphasized the adaptation to future climate change (Carroll et al., 2017) and were mainly controlled by large-scale topographic conditions. According to 20 years of phenological observation, phenology stability reflected the plants' growth cycles synchrony and animal life habits (Menzel et al., 2006; Thackeray et al., 2010; Reed et al., 2013). Therefore, the climate refugia in these three aspects complement each other in terms of temporal scale and climate adaptation capacity (Fig. 7). However, our analysis showed that climate refugia using different environmental diversity and climatic velocity indicators, differed from the priorities derived from phenology stability, according to distribution probability along an elevation gradient (Figs. 4 and 5). For instance, the former's highest probability of climate refugia being identified is mainly distributed in low or high elevations,

and the latter is mostly observed at 3000m – 3800m (Fig. 4, 7). This inconsistent distribution of different types of climate refugia weakens this potential for functional complementarity, highlighting the complexity of biological conservation on the TP.

Land cover and topography are key to potential climate refugia. For instance, priorities of landcover diversity were observed in a combination of forest, shrub, and grassland at low elevations such as the Sannan, Nyingchi, and Hengduan mountains. The distribution probability decreases rapidly with elevation, as the land use type shifts to a single type, such as alpine meadows (Fig. 5). Forest at low elevation has a limited warming effect in winter. However, a significant cooling effect in summer (Li et al., 2015), resulted in a divergent distribution of winter and summer LST diversity. Because complex terrain features have steep climatic gradients, they can facilitate local microscale separation from regional climates, potentially mitigating regional climatic exposure (Ashcroft, 2010; Dobrowski, 2011). For instance, when cold air moves from higher elevations and gathers in valley bottoms, incised valleys squint towards temperature inversions, increasing the resistance to the rising regional temperatures (Dobrowski, 2011). North-facing slopes can buffer the impact of temperature change, for mean annual temperature differences of 6 °C between north- and south-facing slopes of steep mountainous terrain (Gruber et al., 2004). Therefore, higher distribution probability based on elevation diversity was mainly found at low (< 3000 m) and high elevations (> 6000 m), as shown in Fig. 4.

The high distribution probability of the two climatic velocity indicators was also concentrated at elevations above 6000 m (Fig. 4). This is due to air temperature decreasing predictably with elevation. The species at the bottom of a hill tend to move uphill to maintain their thermal conditions as the climate warms. However, conversely, flat regions have more homogenous thermal conditions, and the species need to move a considerable distance to locate a suitable thermal environment, which would manifest as a high climatic velocity (Brito-Morales et al., 2018). The phenology stability difference in low- and high-elevation regions may be related to precipitation change. Previous research has indicated that water availability restricts plant growth in arid areas (Jeong et al., 2011; Shen et al., 2011), and the large-scale atmospheric circulation systems can influence precipitation. According to local stations observation, surface wind speed fluctuations were stronger in regions with a higher elevation than in lower-elevation environments (Guo et al., 2016), and it possibly leads to larger precipitation variations in higher-elevation, further disturbing the phenology stability.

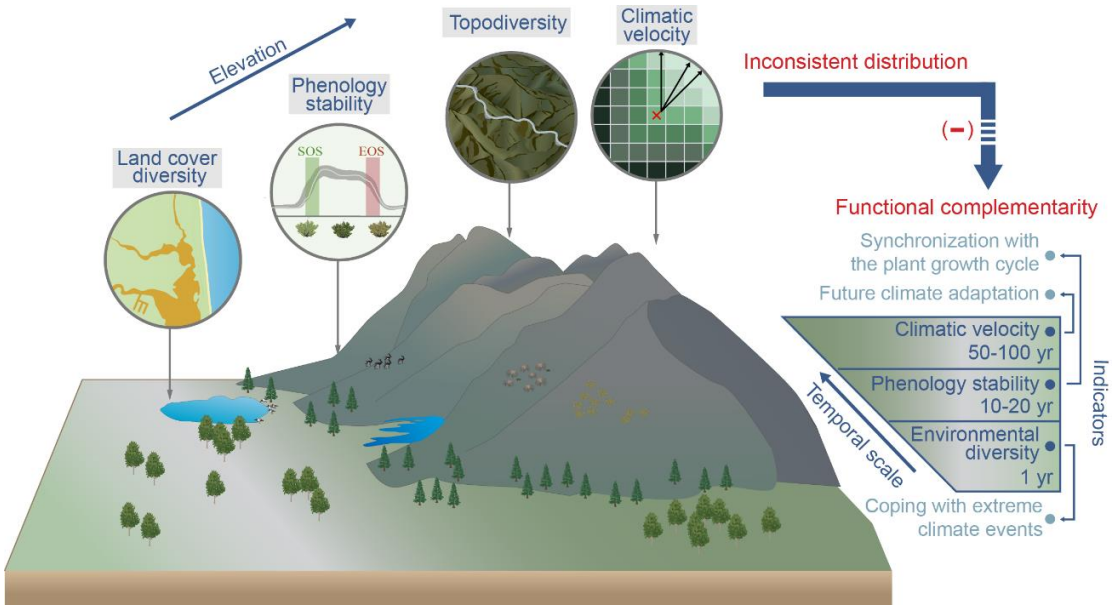

Figure 7. Distribution mode of different types of climate refugia and their ability to buffer the climate change effects.

4.2 Conservation gaps in existing PAs for climate refugia

Conservation efforts in China started late, and the NRs are an emergency solution to avert biodiversity loss and ecosystem degradation (Huang et al., 2019). However, the quick creation of part NRs lacked systematic and coherent conservation planning, which is essential for maximizing protection targets' effectiveness and representativeness (Wu et al., 2011). The low coverage of PAs for climate refugia is a typical example (Fig. 5). The current distribution of NRs on the TP covered a limited proportion of climate refugia (9.9%-25.2%). The proportion of protected land that can buffer climate change impacts ranges from 7.3%-17.8% (Fig. 5). This shows that most of the protected land has a limited capacity to protect itself from extreme weather events or future climate change, even in the core zones of NRs (Fig. S8). It illustrated that the rapid establishment of PAs on the TP has not properly incorporated climate refugia into their planning.

The low coverage is primarily due to a spatial mismatch between NRs locations and climate refugia. NRs are mainly distributed in the northwest, but climate refugia are mostly distributed in the southeast. For instance, Chang Tang, Altun, and Hoh Xil, three large-size NRs located in the northwest, account for 54.4% of the entire reserve areas on the TP and 15.2% of the entire TP, but they cover only a limited number of the climate refugia (0% to 4.6%) based on different indicators. The NRs located in the southeast of the TP, although numerous, are small and fragmented, still hardly forming an effective coverage of climate refugia. Also, previous works reported that the quantity and spatial allocation of PAs on the TP are short regarding biodiversity conservation goals and ecosystem services supply (Xu et al., 2017; Zhang et al., 2018; Li et al., 2020). The notable conservation gaps mean that the current NRs cannot effectively protect these hotspots with crucial

ecological value. NRs are the strictest management type of PAs in China, and resource exploitation inside NRs is severely limited. It implies that the establishment of inefficient NRs squeezes the productive space of local people, which in turn affects their livelihood. Together with our results, these analyses highlight the urgency to optimize PAs on the TP. And the low coverage of climate refugia in NRs was also observed in North America, which highlights that climate refugia values were not fully understood in current conservation planning (Michalak et al., 2018; Stralberg et al., 2020).

4.3 Limitations and uncertainty

Some limitations and uncertainties should be further addressed in this study. First, the climatic velocity approach, which is species-neutral, does not account for the climatic requirements of individual species due to data availability. We assumed that areas with low climatic velocity are appropriate refugia. However, likely, different species would respond differently to the same disturbance. Therefore, future works need to consider these aspects, especially flagship species (e.g., Tibetan antelope and the giant panda). Second, our analysis is also affected by limitations stemming from data resolution. For example, data with different resolutions were used, especially the resolution of DEM (30 m) is quite different from others (500/1000m). Previous studies also mentioned these limitations (e.g., Gomes et al., 2021). Another concern is the uncertainty of climate models (e.g., Wootten et al., 2017). The climate refugia identification may inherit the uncertainties of these models, even though the multi-model ensemble mean of 8 climate models is used to mitigate this concern.

4.4 Ecological and policy implications

Most of the climate refugia sites were identified in TP southeastern area (Fig. 3). Our results showed that the current NRs do not cover a large climate refugia potential area (Fig. 5). Therefore, it is key to expand the NRs to territories with a high climate refugia potential. This will improve PAs effectiveness. Our work identified these areas and recommended establishing NRs clusters in these priority areas, such as Sannan, Nyingchi, Qamdo, and Garz. One approach is to merge multiple small-size and fragmented NRs, which would solve the problem of insufficient habitat connectivity and isolation. Furthermore, given the moderately high overlap between biodiversity, ecosystem services, and climate refugia (Xu et al., 2017; Zhang et al., 2018; Li et al., 2020), expanding NRs in these regions can help protect more sources with high ecological value. The results showed that the high distribution probability of terrain-based/velocity-based indicators is concentrated in high elevations (Fig. 4). This particular type of climate refugia will be a low-cost adaptation strategy for low accessibility, low land use cost, and less potential for agricultural development and resources exploitation (Joppa & Pfaff, 2009).

The applicability and efficiency of future conservation strategy also affected by the interactions between climate change and extensive land use (Alagador et al., 2014; Maxwell et al., 2019). Indeed, a sizable part of the climate refugia identified is predicted to be located southeast of the study area. Better hydrothermal conditions and increased food demand are likely to accelerate agricultural development in this region. The agricultural reclamation and forestry operations may further negatively affect species to track the climate niche movement (Ordonez et al., 2014) and thus increase extinction risks (Hansen et al., 2020; Pillay et al., 2022). Therefore, future climate adaptation strategies should include specific types of agricultural land, such as cropland with high nature value (Doxa et al., 2010, 2012), and focus on the agricultural areas connected to PA networks (Kleijn et al., 2020).

Our work also supported the development of the first national park system in China. The Chinese government is seeking to establish a national park system and the Third Pole National Park Group in this region. If resources and funds permit, we suggest incorporating these prior climate refugia in the conservation planning of the national parks system. Although our analysis identifies areas that help species adapt to climate change as candidates for conservation planning, we do not suggest that regions with a low proportion of climate refugia should be ignored. In such areas, including Hoh Xil and Selinco NRs, continuous monitoring and proactive intervention (e.g., increasing habitat connectivity) may be appropriate conservation measures (Gillson et al., 2013; Kong et al., 2021).

Several promising proposals are being planned for post-2020. For instance, the post-2020 Convention on Biological Diversity framework embraced the goal of "reducing threats". Therefore, it is paramount to integrate climate adaptation considerations into PA's planning and management (Tittensor et al., 2019). Furthermore, according to the UN declaration of "a Decade on Ecosystem Restoration", 350 million hectares of degraded land are scheduled to be restored by 2030 (UN Environment Agency, 2019). The Chinese government has further improved the compensation mechanism for ecological protection. A nationwide pilot plan for comprehensive ecological compensation has encompassed twenty-three counties in TP (National Development and Reform Commission of China, 2019). These restoration efforts will favour species conservation, restoration of natural communities, and enhance their climate resilience (Ordonez et al., 2014; Asamoah et al., 2021). Furthermore, SDG13 (Climate Action), SDG 15 (Life on Land), and other related targets of SDGs framework (e.g., 13.2, 15.5, and 15.9) also advocated for tangible actions to improve the climate resilience, as well as the integration of these goals into conservation planning (UN, 2015). Incorporating climate refugia into PAs planning can be a solution to promote these goals.

5 Conclusion

Given the challenges associated with conserving biodiversity in a changing climate, conservation planning should consider climate refugia to mitigate the climate change effect on species extinction. The identification methods that combine various physical and ecological processes can provide more nuanced depictions of the usefulness of climate refugia. This study compared several climate refugia based on diverse indicators and assessed how they are distributed in NRs on the TP. The climate refugia identified by environmental diversity, climatic velocity, and phenology stability indicators differed substantially, indicating the possible absence of functional complementarity of climate adaptation. Furthermore, existing NRs have notable conservation gaps for these refugia identified, particularly in the southeastern part of TP. It highlighted the urgency of strengthening PAs for climate refugia on the TP. Our work provides a comprehensive understanding of climate refugia, which can support better climate-driven conservation policies in the face of global warming.

References

Ackerly, D.D., Loarie, S.R., Cornwell, W.K., Weiss, S.B., Hamilton, H., Branciforte, R., Kraft, N.J.B., 2010. The geography of climate change: Implications for conservation biogeography. Divers. Distrib. 16, 476–487.

Alagador, D., Cerdeira, J.O., Araújo, M.B., 2014. Shifting protected areas: Scheduling spatial priorities under climate change. J. Appl. Ecol. 51, 703–713.

Asamoah, E.F., Beaumont, L., Maina, J., 2021. Climate and land-use changes reduce the benefits of terrestrial protected areas. Nat. Clim. Chang. 11.

Ashcroft, M., 2010. Identifying refugia from climate change. J. Biogeogr. 37, 1407–1413.

Brito-Morales, I., Molinos, J., Schoeman, D., Burrows, M., Poloczanska, E., Brown, C., Ferrier, S., Harwood, T., Klein, C., McDonald-Madden, E., Moore, P., Pandolfi, J., Watson, J., Wenger, A., Richardson, A., 2018. Climate Velocity Can Inform Conservation in a Warming World. Trends Ecol. Evol. 33.

Carroll, C., Roberts, D., Michalak, J., Lawler, J., Nielsen, S., Stralberg, D., Hamann, A., McRae, B., Wang, T., 2017. Scale-dependent complementarity of climatic velocity and environmental diversity for identifying priority areas for conservation under climate change. Glob. Chang. Biol. 23.

Chen, J., Jönsson, P., Tamura, M., Gu, Z., Matsushita, B., Eklundh, L., 2004. A simple method for reconstructing a high-quality NDVItime-series data set based on the Savitzky–Golay filter. Remote Sens. Environ. 91 (3–4), 332–344.

Cong, N., Piao, S., Chen, A., Wang, X., Lin, X., Chen, S., Han, S., Zhou, G., Zhang, X., 2012.

537 Spring vegetation green-up date in China inferred from SPOT NDVI data: A multiple model analysis.
538 Agric. For. Meteorol. 165, 104–113.
539 Dobrowski, S., Littlefield, C., Lyons, D., Hollenberg, C., Carroll, C., Parks, S., Abatzoglou, J.,
540 Hegewisch, K., Gage, J., 2021. Protected-area targets could be undermined by climate change-
541 driven shifts in ecoregions and biomes. Commun. Earth Environ. 2, 198.
542 Dobrowski, S.Z., 2011. A climatic basis for microrefugia: the influence of terrain on climate.
543 Glob Change Biol 17: 1022–35.
544 Doxa, A., Bas, Y., Paracchini, M.-L., Pointereau, P., Terres, J.-M., Jiguet, F., 2010. Low-
545 intensity agriculture increases farmland bird abundances in France. J. Appl. Ecol. 47, 1348–1356.
546 Doxa, A., Paracchini, M.-L., Pointereau, P., Devictor, V., Jiguet, F., 2012. Preventing biotic
547 homogenization of farmland bird communities: The role of High Nature Value farmland. Agric.
548 Ecosyst. Environ. 148, 83–88.
549 Elsen, P.R., Farwell, L.S., Pidgeon, A.M., Radeloff, V.C., 2020. Landsat 8 TIRS-derived
550 relative temperature and thermal heterogeneity predict winter bird species richness patterns across
551 the conterminous United States. Remote Sens. Environ. 236
552 Elsen, P.R., Farwell, L.S., Pidgeon, A.M., Radeloff, V.C., 2021. Contrasting seasonal patterns
553 of relative temperature and thermal heterogeneity and their influence on breeding and winter bird
554 richness patterns across the conterminous United States. Ecography 1–13.
555 Farwell, L.S., Elsen, P.R., Razenkova, E., Pidgeon, A.M., Radeloff, V.C., 2020. Habitat
556 heterogeneity captured by 30-m resolution image texture predicts bird richness across the
557 conterminous USA. Ecol. Appl. 30 https://doi.org/10.1002/eap.2157.
558 Ganguly, S., Friedl, M.A., Tan, B., Zhang, X.Y., Verma, M., 2010. Land surface phenology
559 from MODIS: characterization of the collection 5 global land cover dynamics product. Remote Sens.
560 Environ. 114 (8), 1805–1816.
561 Garcia, R. A., Cabeza, M., Rahbek, C. & Araujo, M. B. 2014. Multiple dimensions of climate
562 change and their implications for biodiversity. Science 344, 1247579–1247579.
563 Gillson, L., Dawson, T. P., Jack, S., & McGeoch, M. A. 2013. Accommodating climate change
564 contingencies in conservation strategy. Trends in Ecology & Evolution, 28, 135–142.
565 Gomes, E., Inácio, M., Bogdzevič, K., Kalinauskas, M., Karnauskaitė, D., Pereira P., 2021.
566 Future scenarios impact on land use change and habitat quality in Lithuania. Environ Res
567 197:111101
568 Gonçalves-Souza, D., Vilela, B., Phalan, B., Dobrovolski, R., 2021. The role of protected areas
569 in maintaining natural vegetation in Brazil. Sci. Adv. 7.
570 Groves CR, Game ET, Anderson MG, et al. 2012. Incorporating climate change into systematic
571 conservation planning. Biodivers Conserv 21: 1651–71.

572 Gruber, S., Hoelzle, M., Haeberli, W., 2004. Rock-wall temperatures in the Alps: modelling
573 their topographic distribution and regional differences. Permafrost Periglac 15: 299–307.
574 Guo, X.Y., Wang, L., Tian, L.D., Li, X.P., 2016. Elevation-dependent reductions in wind speed
575 over and around the Tibetan Plateau. Int. J. Climatol. 36, doi: 10.1002/joc.4727.
576 Hamann, A., Roberts, D.R., Barber, Q.E., Carroll, C. Nielsen, S.E., 2015. velocity of climate
577 change algorithms for guiding conservation and management. Glob. Change. Biol, 21: 997-1004.
578 Hoffmann, S., Irl, S.D.H. & Beierkuhnlein, C., 2019. Predicted climate shifts within terrestrial
579 protected areas worldwide. Nat. Commun. 10, 4787. https://doi.org/10.1038/s41467-019-12603-w
580 Huang, Y., Fu, J., Wang, W., Li, J., 2019. Development of China's nature reserves over the past
581 60 years: An overview. Land Use Policy 80, 224–232.
582 IPCC., 2014. Climate change 2014: impacts, adaptation and vulnerability. In: Summary for
583 Policy Makers. Contribution of Working Group II to the Fifth Assessment Report of the
584 Intergovernmental Panel on Climate Change (eds. Field CB, Barros VR, Dokken DJ, Mach KJ,
585 Mastrandrea MD, Bilir TE, Chatterjee M, Ebi KL, Estrada YO, Genova RC, Girma B, Kissel ES,
586 Levy AN, MacCracken S, Mastrandrea PR, White LL), pp. 1–32. Cambridge University Press,
587 Cambridge, UK.
588 Jeong, S.J., Ho, C.-H., Brown, M., Kug, J.-S., Piao, S., 2010. Browning in desert boundaries
589 in Asia in recent decades. J. Geophys. Res. 116, D02103.
590 Joppa, L. N., & Pfaff, A., 2009. High and far: Biases in the location of protected areas. PLoS
591 One, 4(12), 1–6.
592 Keppel, G., Van Niel, K.P., Wardell-Johnson, G.W., Yates, C.J., Byrne, M., Mucina, L., Schut,
593 A.G.T., Hopper, S.D., Franklin, S.E., 2012. Refugia: Identifying and understanding safe havens for
594 biodiversity under climate change. Glob. Ecol. Biogeogr. 21, 393–404.
595 Kleijn, D., Biesmeijer, K., Klaassen, R., Oerlemans, N., Raemakers, I., Scheper, J., Vet, L.,
596 2020. Integrating biodiversity conservation in wider landscape management: Necessity,
597 implementation and evaluation, in: Advances in Ecological Research. pp. 127–159.
598 Kong, L., Xu, W., Xiao, Y., Pimm, S., Shi, H., Ouyang, Z., 2021. Spatial models of giant pandas
599 under current and future conditions reveal extinction risks. Nat. Ecol. Evol. 5, 1–8.
600 Kuang, X., Jiao, J., 2016. Review on climate change on the Tibetan Plateau during the last half
601 century. J. Geophys. Res. Atmos. 121.
602 Lawler, J.J., Ackerly, D.D., Albano, C.M., Anderson, M.G., Dobrowski, S.Z., Gill, J.L., Heller,
603 N.E., Pressey, R.L., Sanderson, E.W., Weiss, S.B., 2015. The theory behind, and the challenges of,
604 conserving nature's stage in a time of rapid change. Conserv. Biol. 29, 618–629.
605 https://doi.org/10.1111/cobi.12505
606 Levin, N., Shmida, A., Levanoni, O., Tamari, H., Kark, S., 2007. Predicting mountain plant

richness and rarity from space using satellite-derived vegetation indices. Divers. Distrib. 13, 692–703.

Li, S., Zhang, H., Zhou, X., Yu, H., Li, W., 2020. Enhancing protected areas for biodiversity and ecosystem services in the Qinghai–Tibet Plateau. Ecosyst. Serv. 43, 101090.

Loarie, SR., Duffy, P.B., Hamilton, H., Asner, G.P., Field, C.B., Ackerly, D.D., 2009. The velocity of climate change. Nature, 462, 1052–1055.

Malika, V.S., Lindsey, G., Katherine, J.W., 2009. How does spatial heterogeneity influence resilience to climatic changes? Ecological dynamics in southeast Madagascar. Ecol. Monogr. 79, 557–574.

Maxwell, S., Reside, A., Trezise, J., McAlpine, C., Watson, J., 2019. Retention and restoration priorities for climate adaptation in a multi-use landscape. Glob. Ecol. Conserv. 18, e00649.

Meddens, A.J.H., Kolden, C.A., Lutz, J.A., et al. 2018. Fire refugia: what are they, and why do they matter for global change? BioScience 68: 944–54.

Menzel, A., Sparks, T.H., Estrella, N., Roy, D.B., 2006. Altered geographic and temporal variability in phenology in response to climate change. Glob. Ecol. Biogeogr. 15, 498–504.

Michalak, J.L., Lawler, J.J., Roberts, D.R., Carroll, C., 2018. Distribution and protection of climatic refugia in North America. Conserv. Biol. 32, 1414–1425.

Michalak, J.L., Stralberg, D., Cartwright, J.M., Lawler, J.J., 2020. Combining physical and species-based approaches improves refugia identification. Front. Ecol. Environ. 18, 254–260.

Morelli, T. L., Daly, C., Dobrowski, S. Z., Dulen, D. M., Ebersole, J. L., Jackson, S. T., et al., 2016. Managing climate change refugia for climate adaptation. PLoS One 11, 1–17.

National Development and Reform Commission of China, 2019. Circular of the National Development and Reform Commission on printing and distributing the Pilot Program for Comprehensive Ecological Compensation. https://www.ndrc.gov.cn/xxgk/zcfb/tz/201911/t20191120_1204116.html?code=&state=123

Oliver, T., Roy, D.B., Hill, J.K., Brereton, T., Thomas, C.D., 2010. Heterogeneous landscapes promote population stability. Ecol. Lett. 13, 473–484.

Ordonez, A., Martinuzzi, S., Radeloff, V.C. & Williams, J.W., 2014. Combined speeds of climate and land-use change of the conterminous US until 2050. Nat. Clim. Change 4, 811–816.

Pecl, G., Araújo, M., Bell, J., Blanchard, J., Bonebrake, T., Chen, I.-C., Clark, T., Colwell, R., Danielsen, F., Evengård, B., Falconi, L., Ferrier, S., Frusher, S., Garcia, R., Griffis, R., Hobday, A., Janion, C., Jarzyna, M., Jennings, S., Williams, S., 2017. Biodiversity redistribution under climate change: Impacts on ecosystems and human well-being. Science, 355.

Piao, S., Fang, J.Y., Zhou, L.M., Ciais, P., Zhu, B., 2006. Variations in satellite-derivedphenology in China's temperate vegetation. Global Change Biol. 12 (4), 672–685.

Plard, F., Gaillard, J.M., Coulson, T., Hewison, A.J.M., Delorme, D., Warnant, C., Bonenfant, C., 2014. Mismatch Between Birth Date and Vegetation Phenology Slows the Demography of Roe Deer. PLoS Biol. 12, 1–8.

Reed, T.E., Grotan, V., Jenouvrier, S., Saether, B., Visser, M.E., 2013. Population growth in a wild bird is buffered against phenological mismatch. Science 340, 488–491.

Shen, M., Tang, Y., Chen, J., Zhu, X., Zheng, Y., 2011. Influences of temperature and precipitation before the growing season on spring phenology in grasslands of the central and eastern Qinghai-Tibetan Plateau. Agric. For. Meteorol. 151, 1711-1722.

Shen, M., Zhang, G., Cong, N., Wang, S., Kong, W., Piao, S., 2014. Increasing altitudinal gradient of spring vegetation phenology during the last decade on the Qinghai-Tibetan Plateau. Agric. For. Meteorol. 189–190, 71–80.

Silveira, E.M.O., Radeloff, V.C., Martinuzzi, S., Martínez Pastur, G.J., Rivera, L.O., Politi, N., Lizarraga, L., Farwell, L.S., Elsen, P.R., Pidgeon, A.M., 2021. Spatio-temporal remotely sensed indices identify hotspots of biodiversity conservation concern. Remote Sens. Environ. 258, 112368.

Stein, A., Gerstner, K., & Kreft, H., 2014. Environmental heterogeneity as a universal driver of species richness across taxa, biomes and spatial scales. Ecology Letters, 17, 866–880.

Stralberg, D., Arseneault, D., Baltzer, J.L., Barber, Q.E., Bayne, E.M., Boulanger, Y., Brown, C.D., Cooke, H.A., Devito, K., Edwards, J., Estevo, C.A., Flynn, N., Frelich, L.E., Hogg, E.H., Johnston, M., Logan, T., Matsuoka, S.M., Moore, P., Morelli, T.L., Morissette, J.L., Nelson, E.A., Nenzén, H., Nielsen, S.E., Parisien, M.A., Pedlar, J.H., Price, D.T., Schmiegelow, F.K.A., Slattery, S.M., Sonnentag, O., Thompson, D.K., Whitman, E., 2020. Climate-change refugia in boreal North America: what, where, and for how long? Front. Ecol. Environ. 18, 261–270.

Stralberg, D., Carroll, C., Nielsen, S.E., 2020. Toward a climate-informed North American protected areas network: Incorporating climate-change refugia and corridors in conservation planning. Conserv. Lett. 13, 1–10.

Studer, S., Stockli, R., Appenzeller, C., Vidale, P.L., 2007. A comparative study of satellite and ground-based phenology. Int. J. Biometeorol. 51 (5),405–414.

Thackeray, S.J., Sparks, T.H., Frederiksen, M., Burthe, S., Bacon, P.J., Bell, J.R., Botham, M.S., Brereton, T.M., Bright, P.W., Carvalho, L., Clutton-Brock, T., Dawson, A., Edwards, M., Elliott, J.M., Harrington, R., Johns, D., Jones, I.D., Jones, J.T., Leech, D.I., Roy, D.B., Scott, W.A., Smith, M., Smithers, R.J., Winfield, I. J., Wanless, S., 2010. Trophic level asynchrony in rates of phenological change for marine, freshwater and terrestrial environments. Glob. Chang. Biol. 16, 3304–3313.

Tittensor, D., Beger, M., Boerder, K., Boyce, D., Cavanagh, R., Cosandey-Godin, A., Ortuno Crespo, G., Dunn, D., Ghiffary, W., Grant, S., Hannah, L., Halpin, P., Harfoot, M., Heaslip, S.,

Jeffery, N., Kingston, N., Lotze, H., Mcgowan, J., Mcleod, E., Worm, B., 2019. Integrating climate adaptation and biodiversity conservation in the global ocean. Sci. Adv. 5, eaay9969.

UN, 2015. Transforming our world: the 2030 Agenda for Sustainable development (United Nations, 2015).

United Nations Environment Agency. Resolution 73/284: United Nations Decade on Ecosystem Restoration (2021–2030). https://undocs.org/A/RES/73/284 (2019)

White, M.A., Thornton, P.E., Running, S.W., 1997. A continental phenology modelfor monitoring vegetation responses to interannual climatic variability. Global Biogeochem. Cycles 11 (2), 217–234.

Williams, J., Jackson, S., 2007. Novel climates, no-analog communities, and ecological surprises. Front. Ecol. Environ. 5, 475–482.

Wolf, A.A., Zavaleta, E.S., Selmants, P.C., 2017. Flowering phenology shifts in response to biodiversity loss. Proc. Natl. Acad. Sci. U. S. A. 114, 3463–3468.

Wotten, A., Terando, A., Reich, B.J., Boyles, R.P., Semazzi, F., 2017. Characterizing sources of uncertainty from global climate models and downscaling techniques. J. Appl. Meteorol. Climatol. 56:3245–3262

Xu, W., Xiao, Yi, Zhang, J., Yang, W., Zhang, L., Hull, V., Wang, Z., Zheng, H., Liu, J., Polasky, S., Jiang, L., Xiao, Yang, Shi, X., Rao, E., Lu, F., Wang, X., Daily, G.C., Ouyang, Z., 2017. Strengthening protected areas for biodiversity and ecosystem services in China. Proc. Natl. Acad. Sci. U. S. A. 114, 1601–1606.

Yu, H.Y., Luedeling, E., Xu, J.C., 2010. Winter and spring warming result in delayedspring phenology on the Tibetan Plateau. Proc. Natl. Acad. Sci. U.S.A. 107 (51),22151–22156.

Zhang, J., Xu, W., Kong, L., Hull, V., Xiao, Yi, Xiao, Yang, Ouyang, Z., 2018. Strengthening protected areas for giant panda habitat and ecosystem services. Biol. Conserv. 227, 1–8.

Zhang, Q., Kong, D., Shi, P., Singh, V.P., Sun, P., 2018. Vegetation phenology on the Qinghai-Tibetan Plateau and its response to climate change (1982–2013). Agric. For. Meteorol. 248, 408–417.

Zhang, X., Friedl, M., Schaaf, C., 2006. Global vegetation phenology from Moderate Resolution Imaging Spectroradiometer (MODIS): Evaluation of global patterns and comparison with in situ measurements. J. Geophys. Res. 111.

Pillay, R., Venter, M., Aragon-Osejo, J., González-del-Pliego, P., Hansen, A. J., Watson, J. E. M., & Venter, O., 2022. Tropical forests are home to over half of the world's vertebrate species. Frontiers in Ecology and the Environment, 20(1), 10–15.

Hansen, A., Burns, P., Ervin, J., Goetz, S., Hansen, M., Venter, O., Watson, J., Jantz, P., Virnig, A., Barnett, K., Pillay, R., Atkinson, S., Supples, C., Rodriguez-Buritica, S., & Armenteras, D., 2020. A policy-driven framework for conserving the best of Earth's remaining moist tropical forests. Nature Ecology & Evolution, 4, 1–8.

Supplementary materials

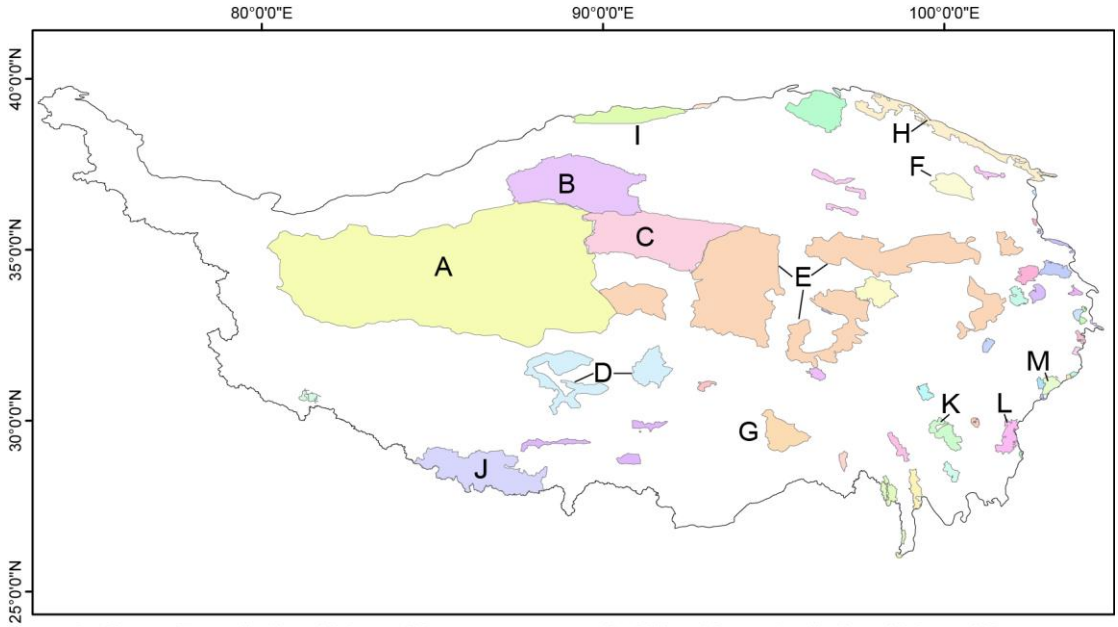

A. Chang Tang National Natural Reserve
B. Altun National Nature Reserve
C. Qinghai Hoh Xil National Nature Reserve
D. Selinco National Nature Reserve
E. Sanjiangyuan National Natural Reserve
F. Qinghai Lake National Nature Reserve
G. Yarlung Zangbu Grand Canyon National Nature Reserve
H. Qilian Mountain National Natural Reserve
I. Lop Nur National Natural Reserve
J. Qomolangma National Nature Reserve
K. Haizishan National Natural Reserve
L. Gongga Mountain National Nature Reserve
M. Wolong National Nature Reserve

Figure S1. Distribution and name of PAs on the Tibetan Plateau. We only marked the names of major national nature reserves.

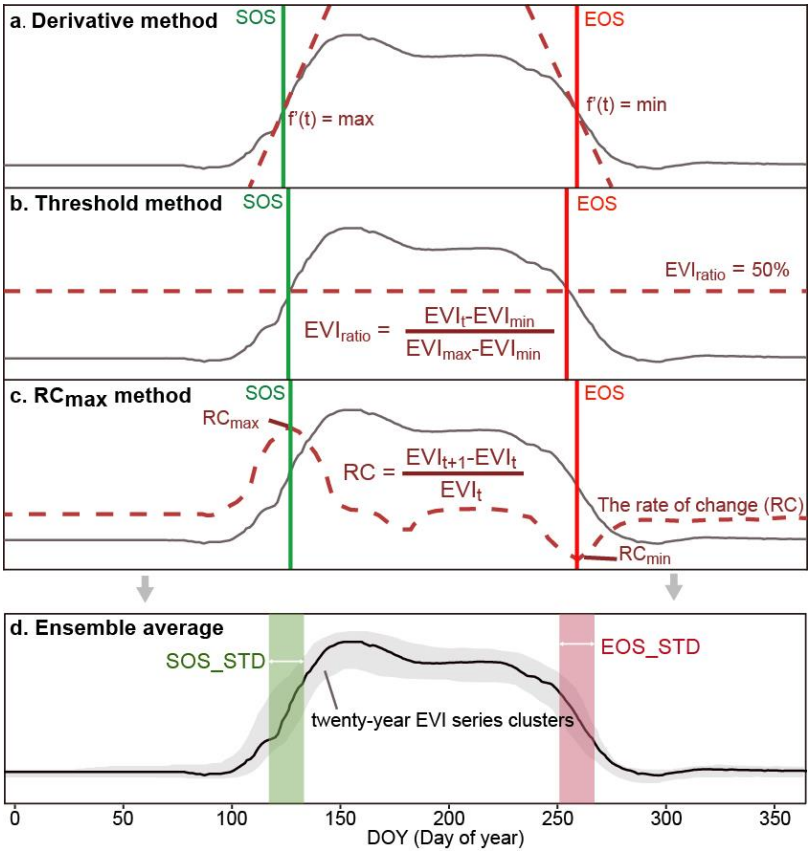

Figure S2. Schematic diagram of phenology calculation. (a-c) indicates the Derivative method, Threshold method, and RC_{max} method, respectively. Start date of the growing season (SOS) and the end date of the growing season (EOS). Please see Section 2.4.2 for the detailed phenology calculation process.

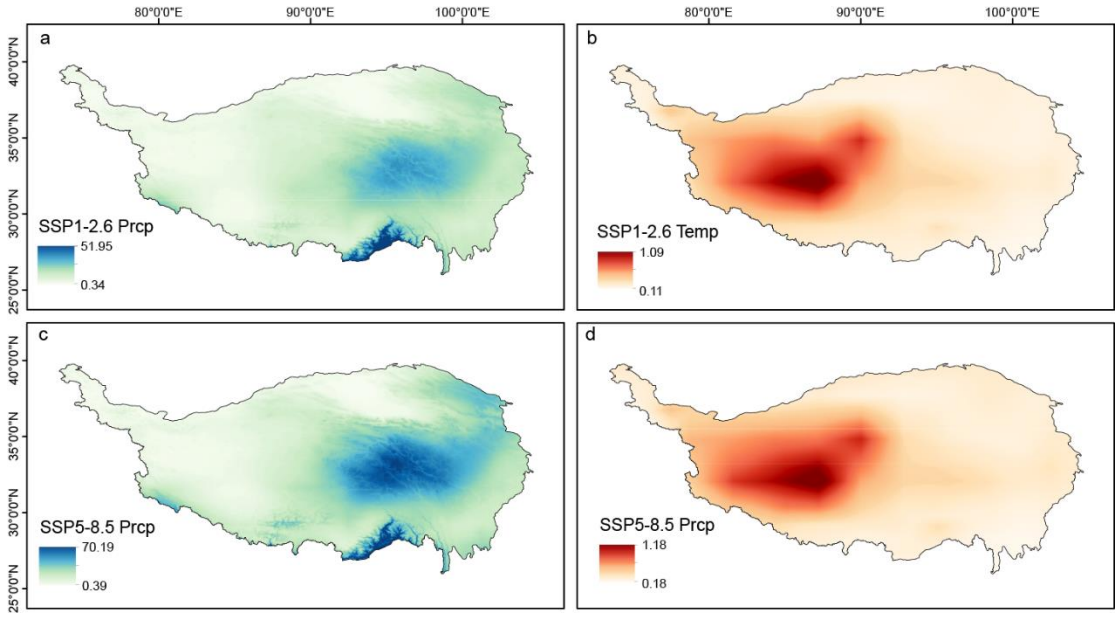

Figure S3. Standard error of future climate under 8 global climate models. “Prcp” means precipitation, and “Temp” means temperature.

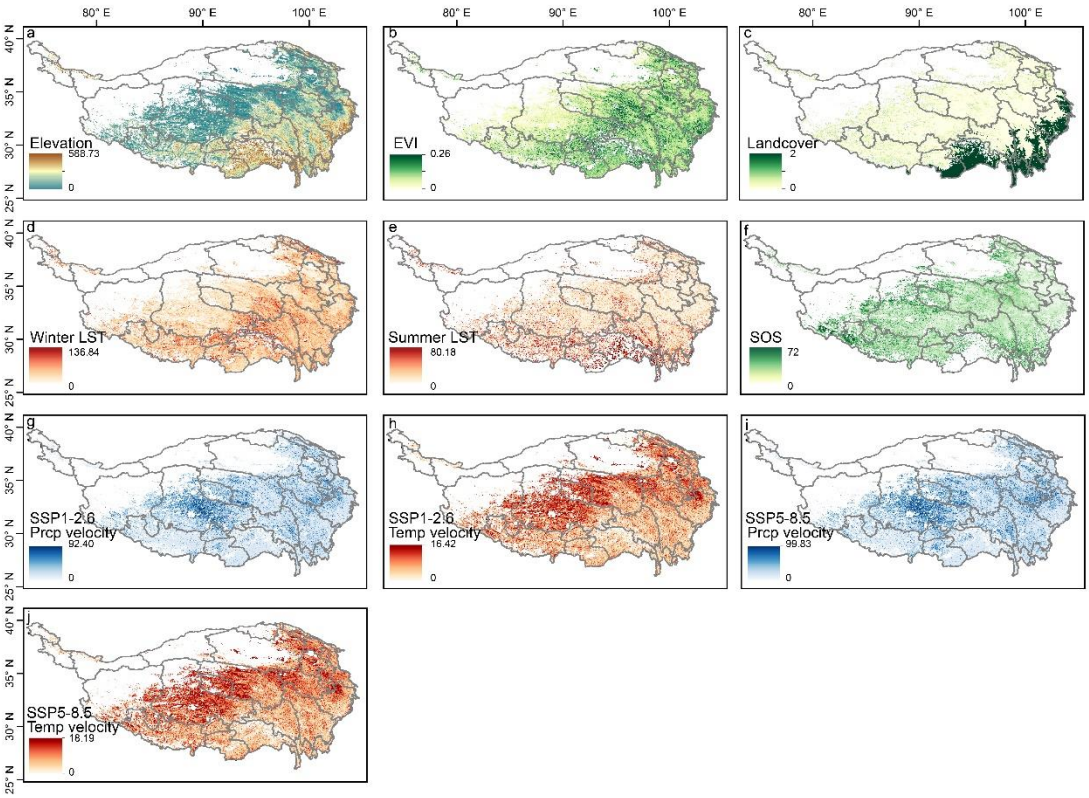

Figure S4. The distribution of climate refugia indicators. “EVI” means enhanced vegetation index, Land surface temperature (LST), precipitation (Prcp), and temperature (Temp), start of the growing season (SOS), and enhanced vegetation index (EVI).

.

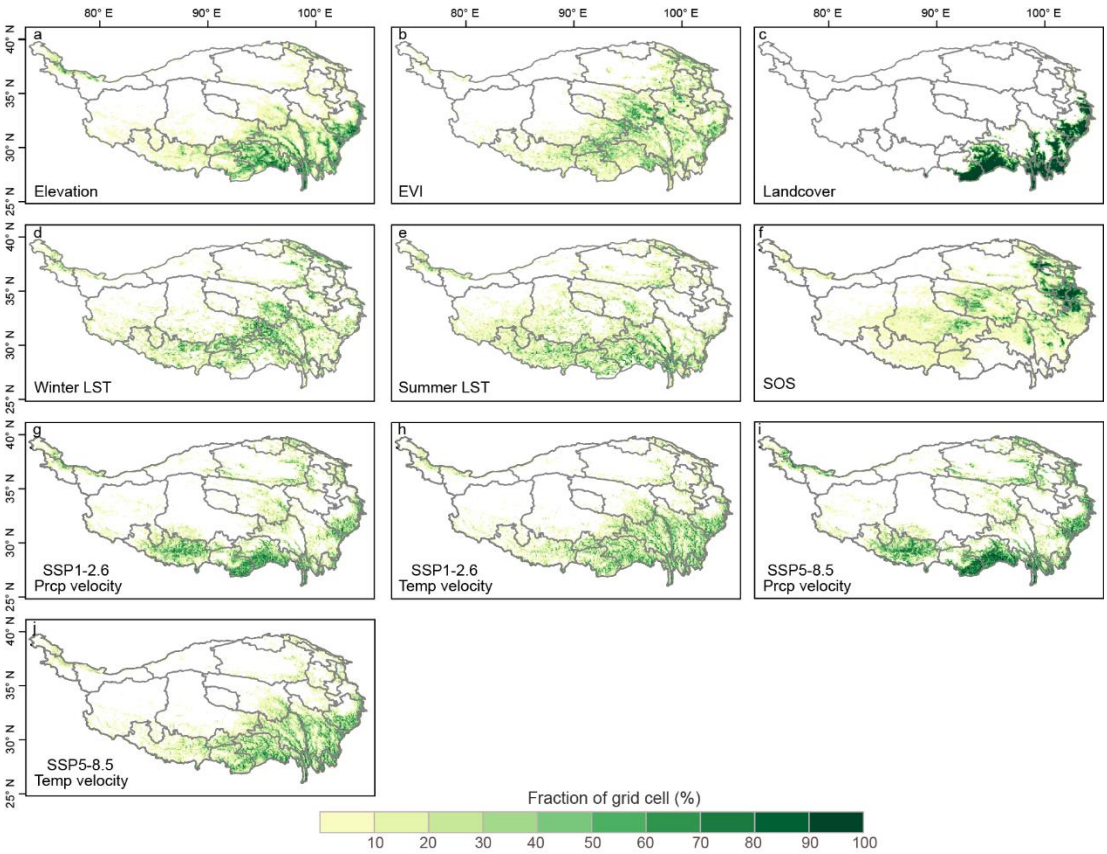

Figure S5. Distribution of priority climate refugia based on different indicators (%) according to **the threshold of 15%**. This figure is part of the sensitivity test with a threshold of 25% (Section 2.5). The figures are aggregated to 0.1 degree resolution for improved visualization. (a-e) showed the environmental diversity of elevation, EVI, landcover, winter LST and summer LST, (f) showed the phenology stability indicator, and (g-j) showed the future climate change velocity for precipitation and temperature for SSP1-2.6 and SSP5-8.5, respectivity. The color shade of green represents the percentage of priority climate refugia. Land surface temperature (LST), precipitation (Prcp), and temperature (Temp), start of the growing season (SOS), and enhanced vegetation index (EVI).

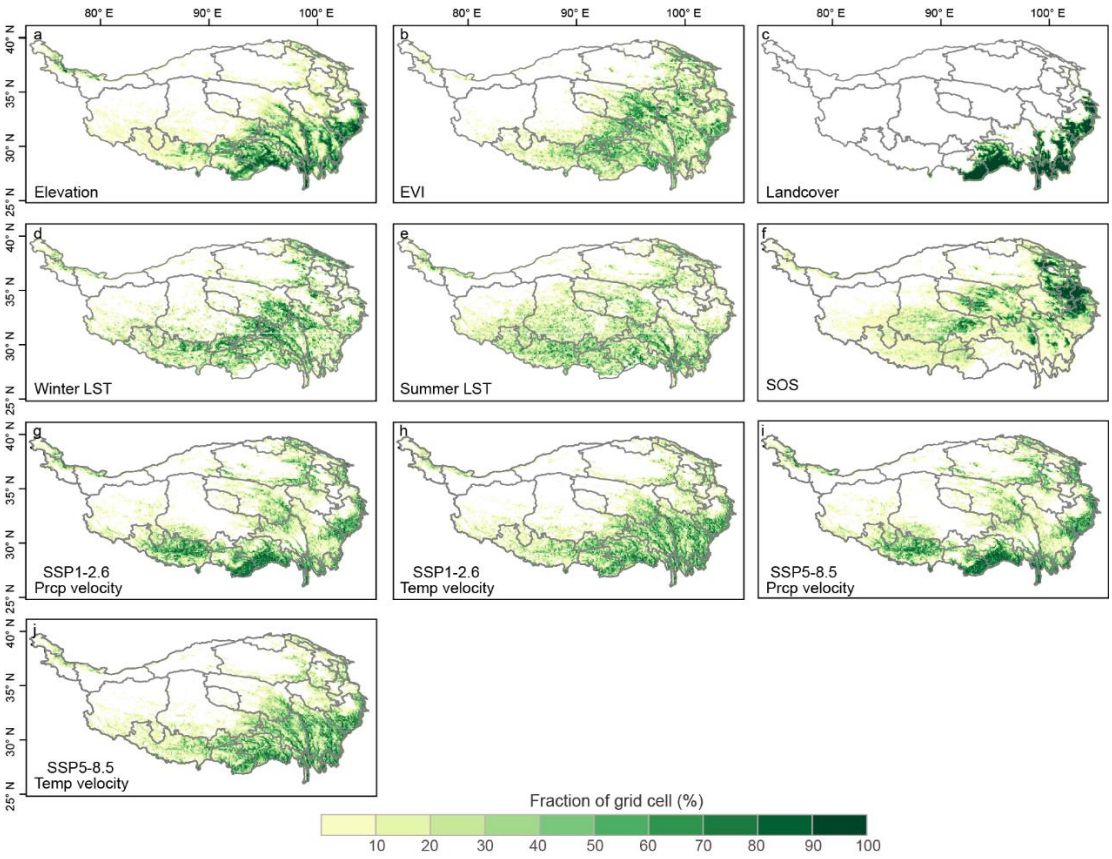

Figure S6. Distribution of priority climate refugia based on different indicators (%) according to **the threshold of 25%**. This figure is part of the sensitivity test with a threshold of 25% (Section 2.5). The figures are aggregated to 0.1 degree resolution for improved visualization. (a-e) showed the environmental diversity of elevation, EVI, landcover, winter LST and summer LST, (f) showed the phenology stability indicator, and (g-j) showed the future climate change velocity for precipitation and temperature for SSP1-2.6 and SSP5-8.5, respectivity. The color shade of green represents the percentage of priority climate refugia. Land surface temperature (LST), precipitation (Prcp), and temperature (Temp), start of the growing season (SOS), and enhanced vegetation index (EVI).

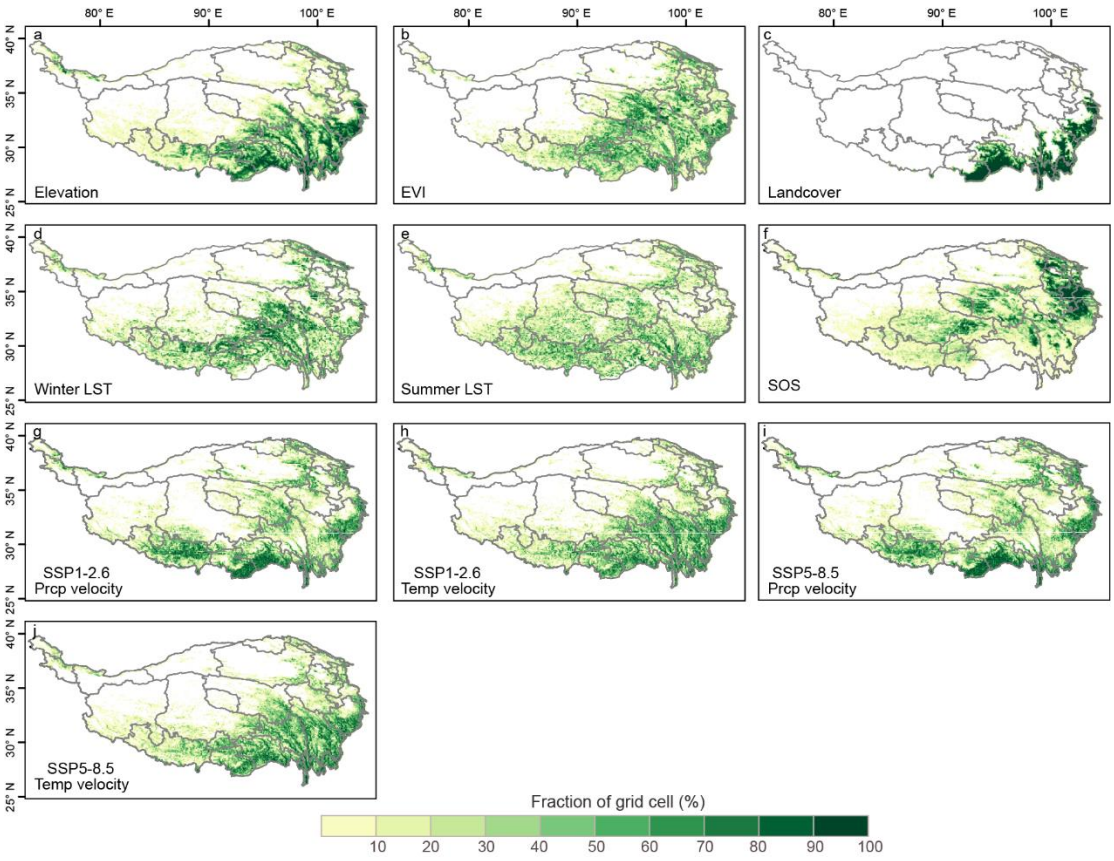

761

762 Figure S7. Distribution of priority climate refugia based on different indicators (%) according to **the**
763 **threshold of 30%**. This figure is part of the sensitivity test with a threshold of 30% (Section 2.5).
764 The figures are aggregated to 0.1 degree resolution for improved visualization. (a-e) showed the
765 environmental diversity of elevation, EVI, landcover, winter LST and summer LST, (f) showed the
766 phenology stability indicator, and (g-j) showed the future climate change velocity for precipitation
767 and temperature for SSP1-2.6 and SSP5-8.5, respectivity.The color shade of green represents the
768 percentage of priority climate refugia. Land surface temperature (LST), precipitation (Prcp), and
769 temperature (Temp), start of the growing season (SOS), and enhanced vegetation index (EVI).

770

771

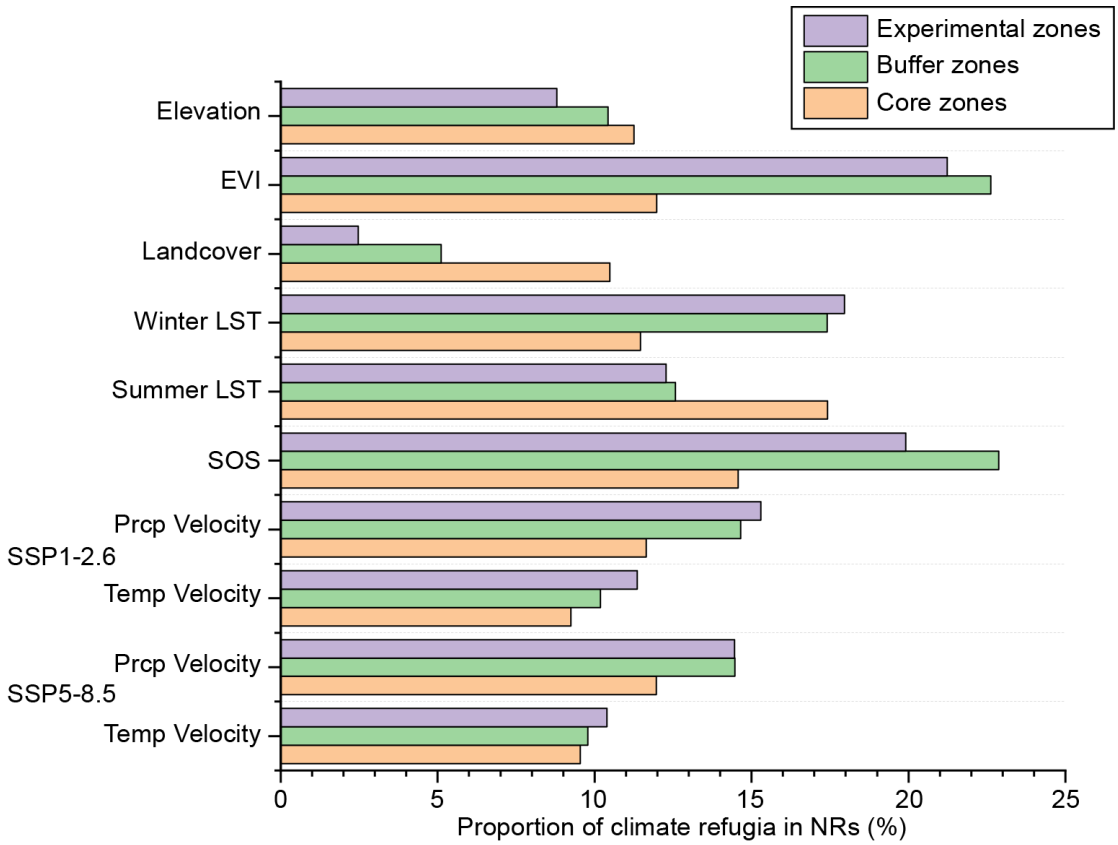

Figure S8. Proportion of climate refugia in different part of NRs: 1) experimental zones, 2) buffer zones, and 3) core zones. Land surface temperature (LST), precipitation (Prcp), and temperature (Temp), and enhanced vegetation index (EVI).